BIODIVERSITAS
Volume 26, Number 11, November 2025
Pages: 5824-5837

ISSN: 1412-033X
E-ISSN: 2085-4722
DOI: 10.13057/biodiv/d261139

Responses of black soybean to rice husk-derived bio-silica nanoparticles and mycorrhiza on physiology and root development under drought stress

DWI SUCI LESTARIANA[1,3], EDI PURWANTO[2,♥], MUJI RAHAYU[2], SUPRIYONO[2]
[1]Doctoral Program in Agriculture Science, Faculty of Agriculture, Universitas Sebelas Maret. Jl. Ir. Sutami 36A, Surakarta 57126, Central Java, Indonesia
[2]Department of Agrotechnology, Faculty of Agriculture, Universitas Sebelas Maret. Jl. Ir. Sutami 36A, Surakarta 57126, Central Java, Indonesia.
Tel./fax.: +62-271-637457, ♥email: edipurwanto@staff.uns.ac.id
[3]Department of Agrotechnology, Faculty of Agriculture and Husbandry, Universitas Boyolali. Jl. Pandanaran 405, Boyolali 57315, Central Java, Indonesia

Manuscript received: 9 September 2025. Revision accepted: 15 November 2025.

Abstract. *Lestariana DS, Purwanto E, Rahayu M, Supriyono. 2025. Responses of black soybean to rice husk-derived bio-silica nanoparticles and mycorrhiza on physiology and root development under drought stress. Biodiversitas 26: 5824-5837.* This study investigated the combined effects of rice husk-derived bio-silica nanoparticles and Arbuscular Mycorrhizal Fungi (AMF) on the physiological and root development responses of two contrasting black soybean (*Glycine max*) cultivars, Malika and Detam 2. A factorial experiment was arranged in a completely randomized design with three replicates. Treatment included two cultivars (Malika, Detam 2), AMF (inoculated, non-inoculated), and five biosilica nanoparticle concentrations (0, 50, 100, 150, 200 ppm). Data were analyzed using ANOVA, and mean differences were compared with Duncan's Multiple Range Test (DMRT). Results showed that cultivar Malika maintained 0.72% ($p<0.05$) lower H_2O_2 accumulation and stronger antioxidant activity, while cultivar Detam 2 exhibited better root development when treated with 150-200 ppm biosilica nanoparticle and combined with AMF inoculation, showing the longest length (37 cm; $p<0.05$) and the greatest volume (3.17 cm^3; $p<0.05$). These improvements indicate that bio silica nanoparticles supported redox stability and osmotic regulation, while AMF strengthened nutrient acquisition and root elongation. Overall, the integrated application of AMF and bio silica nanoparticles induced complementary biochemical and morphological tolerance mechanisms in both cultivars, enhancing drought resilience through reduced oxidative stress, improved osmotic balance, and strengthened root development. This study provides evidence of synergistic interactions between AMF and rice husk-derived bio-silica nanoparticles in black soybean, offering a sustainable, waste-based strategy to improve legume productivity under dryland and climate-stress conditions.

Keywords: Arbuscular mycorrhizal fungi, black soybean, drought stress, rice husk-derived bio-silica nanoparticles, root development

INTRODUCTION

Drought stress is a major abiotic constraints limiting soybean (*Glycine max* (L.) Merr.) productivity, especially in tropical regions dependent on rain-fed agriculture (Luan et al. 2021; Poudel et al. 2023). Water scarcity disrupts plant water balance, root development, nutrient uptake, and oxidative homeostasis, resulting in reduced yield (Arya et al. 2021). These challenges are prominent in Indonesia's dryland ecosystems such as Boyolali District, Central Java, where rainfall variability strongly influences production. In 2020, soybean yield in Boyolali reached only 1,807.5 tons from 1,205 ha, insufficient to meet regional demand (Badan Pusat Statistik Boyolali 2022). Enhancing drought tolerance is therefore essential to stabilize production and support food security.

Black soybean, a local variant of *G. max,* possesses higher protein, anthocyanin, and antioxidant levels than yellow soybean (Bhartiya et al. 2020). Despite its nutritional advantages, its cultivation remains limited due to drought sensitivity. Detam 2 and Malika are two Indonesian black soybean cultivars with contrasting characteristics: Detam 2 contains higher protein (45%) than Malika (37%), while Malika shows better drought tolerance; however, both exhibit similar yield potential of 2.34-2.46 t ha^{-1} (Balitkabi 2024). Improving productivity under marginal conditions requires strategies that strengthen physiological and root related drought responses. Soybean drought resilience is linked to biochemical adjustments, including proline and ascorbate accumulation, and to root system development, which enhances access to deeper soil water (Asadullah et al. 2024; Guo et al. 2024). Understanding how these biochemical and morphological mechanisms interact is critical for developing sustainable strategies for drought adaptation.

Silicon (Si) has emerged as a beneficial element for improving crop tolerance. Nanotechnology-based fertilizers such as Silica Nano-Particles (SiNPs) enhance nutrient efficiency, regulate antioxidant metabolism, and improve water use efficiency under stress (Mathur and Roy 2020; Naidu et al. 2023). However, research on SiNPs has focused on cereal crops such as rice and wheat, which are strong silicon accumulators (Bhat et al. 2021). Legumes, including soybeans, are low silicon accumulators (Putra et al. 2022) and their response to nanosilica remains insufficiently explored. Moreover, few studies have utilized rice husk-derived biosilica nanoparticles, despite their potential for waste valorization in sustainable agriculture. Effective nanosilica concentrations vary across species and application methods, with positive effects observed even at low (Suciaty et al. 2018; Herawati et al. 2021). In the present study, nanosilica was applied at 0, 50, 100, 150, and 200 ppm to capture this potential response range and to determine the most effective dose under drought conditions. The upper limit (200 ppm) was selected to remain well below the phytotoxic threshold (>2000 mg L^{-1}) reported by Lee et al. (2010).

Arbuscular mycorrhizal fungi (AMF) offer another complementary. AMF form symbiotic associations with roots that improve nutrient uptake, root elongation, and stress hormone regulation (Tang et al. 2022; Wadas 2022; Nader et al. 2024; Rakesh et al. 2024). AMF colonization enhances root architecture and activates antioxidant defenses, contributing to greater drought resilience (Hasanuzzaman et al. 2022; Chowdhary and Songachan 2025). Recent studies indicate potential synergistic interaction between AMF and silicon-based amendments, jointly improving plant growth and water status under drought stress (Moradtalab et al. 2019; Wahab et al. 2023). The integration of AMF inoculation with nanosilica aligns with emerging bio-nanotechnological approaches that combine biological symbiosis and nanomaterial based resilient.

Most previous studies have examined either biochemical or morphological parameters separately. Few have simultaneously evaluated antioxidant defense mechanisms (proline, H_2O_2, ascorbic acid, IC_{50}) together with root development within a single framework. Integrating these parameters provides a more comprehensive understanding of drought tolerance and is particularly useful for comparing contrasting cultivars such as Malika and Detam 2.

Although nanosilica and AMF individually show promise in improving drought stress response, their combined effects in low-silicon legumes remain uncertain. The synergistic potensial of rice husk derived biosilica nanoparticle and AMF to strengthen biochemical antioxidant responses and root development under drought condition has not been systematically investigated. Addressing this gap is essential for advancing sustainable agriculture and improving dryland soybean productivity. This study introduces a novel integration of rice husk derived biosilica nanparticles and AMF to enhance drought tolerance in black soybean. Unlike prior studies that evaluated single response categories, this research simultaneously assesses biochemical and root system responses in two contrasting cultivars, highlighting the sustainable and eco friendly potential of waste derived nanosilica within low input agricultural innovation.

MATERIALS AND METHODS

Research location

This research was conducted in a greenhouse located at Faculty of Agriculture and Animal Husbandry, Universitas Boyolali, Boyolali, Indonesia. Meanwhile, the biosilica nanoparticle characterization was carried out at the Integrated Research and Testing Laboratory, Universitas Gadjah Mada, Yogyakarta, Indonesia. The biochemical analysis was also performed at the Plant Physiology and Biotechnology Laboratory, Faculty of Agriculture, Universitas Sebelas Maret, Surakarta, Indonesia.

Synthesis of biosilica nanoparticle from rice husk ash

The synthesis of biosilica nanoparticles is a variation of the method (Dang et al. 2018). Rice husks obtained from milling facilities were incinerated to produce ash, which was sieved using a 120-mesh sieve for uniform particle size. The ash (50 g) was treated with 1 N HCl (500 mL) under stirring for 2 h at room temperature, left to settle overnight, filtered, rinsed with distilled water, and oven-dried at 60°C. The dried ash was then calcined at 700°C for 4 h (modified from the original duration) with an approximate heating rate of 10°C min^{-1} to obtain biosilica nanoparticles. Characterization included TEM (Transmission Electron Microscope), EDX (Energy Dispersive X-ray), XRD (X-ray Diffraction), and FTIR (Fourier Transform Infrared Spectroscopy) analyses to determine morphology, elemental composition, crystallinity, and functional groups, respectively.

Experimental design

The research was designed using a Completely Randomized factorial Design (CRD) with three replicates. The experiment utilized two black soybean cultivars, Malika (drought-tolerant) and Detam 2 (drought-susceptible), which were used with AMF (without inoculation and inoculation); biosilica nanoparticle concentration (0, 50, 100, 150, and 200 ppm). Each polybag contained one soybean (*Glycine max*) plant. For each treatment, nine polybags were prepared, three for biochemical assays, three for root morphology, and three were maintained until maturity for yield analysis. For biochemical analysis, leaves from the three plants per treatment were pooled to form one composite sample.

Plant material and growth conditions

Black soybean cultivation was conducted in greenhouse using polybags. Detam 2 (susceptible) and Malika (tolerant) cultivars selected from previous screening were used. The growing medium consisted of 6 kg of soil and 64 g of cow compost per polybag. The seeds were soaked in a sugar solution (200 g L^{-1}) until swollen, filtered, and inoculated with rhizobium to coat the surface before planting. At planting, commercial endomycorrhizal inoculum treatment Fumyco®. According to the manufacturer's specification, the inoculum contains spores of *Glomus* spp., predominantly with an approximate density of 155 spores per 10 g carrier. The colonization rate of inoculated roots averaged 50%-100% which is classified as a high level of colonization according to (Sitepu et al. 2024) (Supplementary Table 7). The inoculum was mixed into the planting substrate at a rate of 10 g per polybag before sowing. Basal fertilization was performed 7 days after planting with 2.04 g urea, 2.72 g SP-36, and 2.72 g KCl per polybag. The average daily temperature and relative humidity were 32°C and 58%, respectively.

Drought stress treatment and foliar application of biosilica nanoparticles

Drought stress treatments were applied from the V1 (14 Days After Planting/DAP) to the R5 phase (56 DAP). Soil moisture was maintained at 25% of field capacity during the drought treatment period. The soil water content was determined gravimetrically every six days, following a preliminary experiment showing that soil moisture naturally decreased to approximately 25% of field capacity when plants were not watered for six days.

Biosilica nanoparticle fertilizer was applied by spraying the entire leaf surface at treatment-specific concentrations, namely S0 (control, without biosilica nanoparticle application), S1 (50 ppm), S2 (100 ppm), S3 (150 ppm), and S4 (200 ppm). Biosilica nanoparticle fertilization was applied once a week in the morning from 08.00 and 10.00 during the V1 stage (14 DAP) until R5 (56 DAP).

Biochemical analysis

Sample collection

Leaf sampling was conducted at the R1 phase (42 DAP). The samples were fully opened trifoliate leaves, starting from the 3rd to the 5th. The harvested leaves were placed in plastic bags according to each treatment and stored in a refrigerator at -4°C until analysis.

Determination of proline

The proline content was determined following the acid ninhydrin method of Bates et al. (1973) with a minor modification in the sample water bath temperature. Leaf tissue 0.5 g was extracted in 3% sulfosalicylic acid, and the resulting filtrate reacted with acid ninhydrin and glacial acetic acid. After incubation in a water bath at 95°C for 1 hour, the reaction mixture was extracted with 4 mL of toluene, and absorbance was measured at 520 nm using a spectrophotometer. Proline concentration was expressed as µmol g^{-1} fresh weight.

Determination of H_2O_2 content

H_2O_2 content was determined following the method of Velikova et al. (2000). Leaf tissue 0.5 g was homogenized in 5 mL 0.1% Trichloroacetic Acid (TCA) and centrifuged to obtain the supernatant. The reaction mixture contained 0.5 mL of 50 mM potassium phosphate buffer (pH 7.0) and 1 mL of potassium iodide (KI) 1M. After incubation in the dark, absorbance was measured at 390 nm using a UV-Vis spectrophotometer. The H_2O_2 concentration was expressed as µmol g^{-1} fresh weight.

Determination of ascorbic acid

The ascorbic acid was determined with the method of Darmanti et al. (2016). Leaf tissue 0.5 g was extracted in 7% sulfosalicylic acid, and the supernatant was used for analysis. The reaction mixture contained 2 mL of 2% Na_2MoO_4, 2 mL of 0.15 M H_2SO_4, and 1 mL of 15 mM Na_2HPO_4. After 1 hour incubation in a water bath 60°C, absorbance was measured at 660 nm using a UV-Vis spectrophotometer. The ascorbic acid content was expressed as ppm.

Determination IC_{50} of DPPH

The IC_{50} value of DPPH was determined using the DPPH (2,2-diphenyl-1-picrylhydrazyl) radical scavenging assay, following the method of Maliya et al (2019). Leaf tissue (0.05 g) was extracted in methanol, and the supernatant was reacted with 0.1 mM DPPH solution. The reaction mixture was incubated in the dark for 30 minutes, and absorbance was measured at 517 nm using a UV-Vis spectrophotometer. The percentage of radical scavenging activity was calculated, and IC_{50} values were obtained by linear regression analysis of extract concentration versus percent inhibition.

Determination root system

Root sampling was conducted destructively from 14 to 28 DAP. The sample observations included the maximum length and volume.

Data analysis

Data were analyzed using ANOVA (cultivar × AMF × biosilica nanoparticle concentration. Effect size was analyzed using partial eta squared and classified using Cohen (1988). Significant effects of ANOVA ($p<0.05$) were separated using Duncan's Multiple Range Test (DMRT). Analyses were conducted in SPSS version 26.0. Furthermore, correlation analysis was used to determine the strength of the relationship between the observed variables.

RESULTS AND DISCUSSION

Characterization of biosilica nanoparticle

Characterization of biosilica nanoparticles includes 3 aspects, namely the detection of particle size, functional group presence, and elemental purity using TEM, FTIR, and EDX instruments, respectively. Figure 1 shows the outcomes of the nano silica particle size assessment at a scale of 100 nm. The image shows spherical and almost-spherical forms, with the majority of particles measuring under 100 nm, in line with the morphology of amorphous nanosilica. The mean diameter is 58.31 nm, confirming successful synthesis at the nanoscale.

The FTIR test (Figure 2) results show the formation of functional groups signifying the presence of nanosilica. The FTIR band spectrum reports a large absorption band at a peak of 3435.57 cm^{-1} due to surface hydroxyl groups (silanol groups, -Si-OH) and adsorbed moisture. In addition, the bending vibration of water is enhanced by the band at 1630.93 cm^{-1}. The pronounced band at 1101.69 cm^{-1} results from the asymmetric stretching vibration of the Si-O-Si network, indicative of amorphous silica. The symmetric stretching of Si-O-Si and the bending vibration of Si-O bonds are evident at 798.88 cm^{-1} and 468.16 cm^{-1}, respectively. The faint bands at 2927.36 cm^{-1} and 2815.69 cm^{-1} are obtained from organic chemicals during the production process. Minor peaks at 1599.53 cm^{-1} and 1348.94 cm^{-1} signify the existence of trace organic or functional groups in the synthesis process.

The EDX test (Figure 3) reports the presence of Silicon (Si) and Oxygen (O) at mass percentages of 44.39% and 54.40%, respectively. Trace elements, including Na, Mg, Al, K, and Cl, are introduced through chemical reagents or residues during the manufacturing process. The results indicate that the biosilica nanoparticle has a purity of 98.79% by mass, with the carrier element at 1.21%.

The XRD pattern (Figure 4) of the produced biosilica nanoparticle shows broad diffraction peaks centered at 2θ = 21.8°, indicative of amorphous silica. Previous research has shown the presence of a wide diffraction peak (hump) within the range of 2θ = 20°-24° (Maddalena et al. 2019). The result is consistent with the conclusions of previous research. The indeterminate structure is beneficial for applications necessitating a high surface area and reactive silanol groups (Wei et al. 2022).

Recapitulation analysis of varian on biochemical activity parameters

The combined application of biosilica nanoparticle and AMF inoculation influenced both biochemical and root developmental parameters of two black soybean cultivars under drought stress (Table 1, Figures 5-6). Proline is an important osmo-protectant that accumulates under deficit to maintain cell turgor and stabilize proteins and membranes. It accumulates in soybean leaves during drought stress (Singh et al. 2022). Foliar application of biosilica nanoparticles significantly tended to increase proline accumulation, particularly in Detam 2, which exhibited relatively higher levels than Malika, suggesting a stronger osmotic adjustment response (Mwenye et al. 2016). At higher concentrations (150-200 ppm), proline level in Detam 2 declined, suggesting stress mitigation and improved osmotic adjustment, consistent with the role of nanosilica in enhancing drought tolerance (Abdo et al. 2024).

Reactive Oxygen Species (ROS) in plants under stress were assessed via H_2O_2 content. The H_2O_2 concentration was reduced in plants treated with AMF and biosilica nanoparticles, especially at 150-200 ppm. Malika tended to maintain lower H_2O_2 levels than Detam 2, suggesting a possible trend toward stronger redox homeostasis (Wei et al. 2025). These reductions suggest that the combined application of AMF and biosilica nanoparticles may contribute to ROS mitigation, possibly through enhanced antioxidant defense capacity (Rakesh et al. 2024).

Ascorbic acid, a key non-enzymatic antioxidant, increased with AMF inoculation, particularly Malika, reinforcing the role of AMF in boosting ROS detoxification (Chandrasekaran 2022; Rudenko et al. 2023). Although H_2O_2 and ascorbic acid were not significantly correlated, this pattern supports complementary action between enzymatic and non-enzymatic antioxidant pathways (Kang et al. 2022; Lismont et al. 2022). The antioxidant activity expressed as IC_{50} indicated a strong radical scavenging capacity (<50 ppm) across treatment (Kowitcharoen et al. 2018). Malika showed consistently lower IC_{50} values than Detam 2, indicating a trend of higher antioxidant potential, although the difference was not statistically significant. The weak negative correlation between proline and IC_{50} (r = -0.205) implies that increased osmolyte accumulation contributed to antioxidant efficiency (Hosseinifard et al. 2022). Overall, these findings highlight the cultivar-specific synergy between AMF and biosilica nanoparticles in improving biochemical resilience under drought stress.

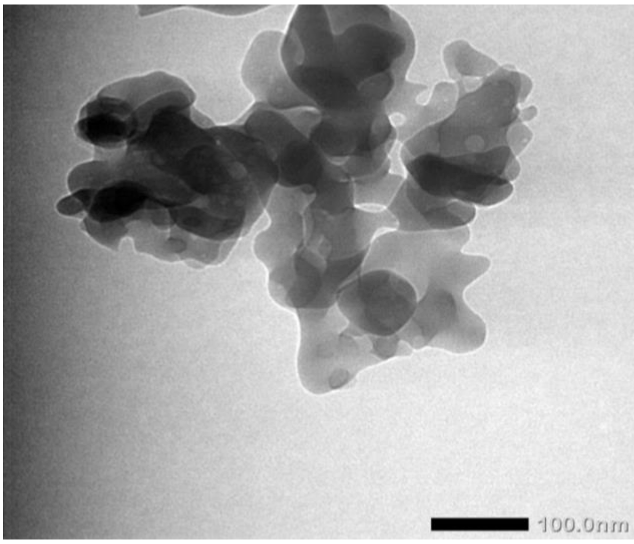

Figure 1. TEM (Transmission Electron Microscope) image of synthesized nanosilica at a scale of 100 nm

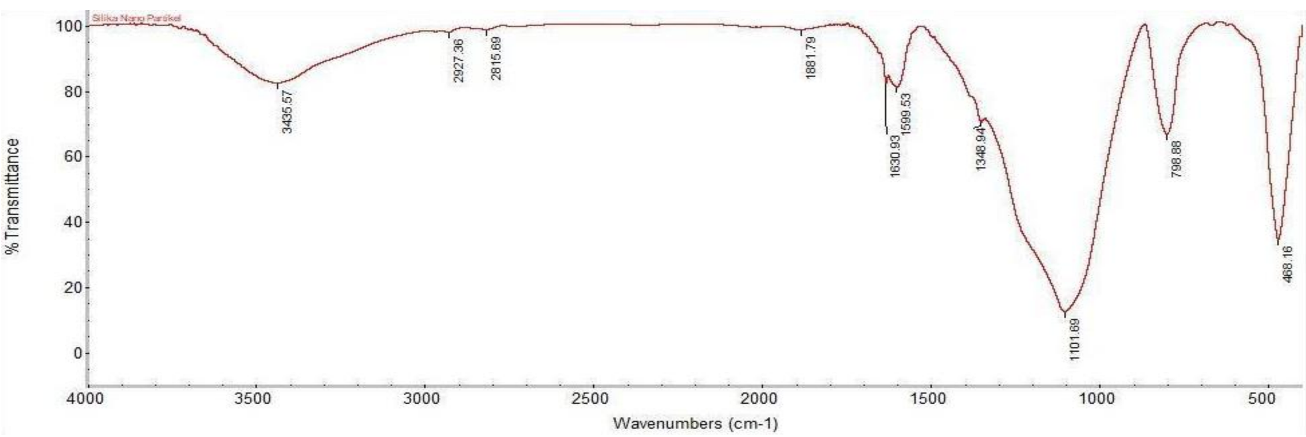

Figure 2. FTIR (Fourier Transform Infrared Spectroscopy) spectrum of nanosilica showing characteristic bands of silanol (3435 cm^{-1}), adsorbed water (1630 cm^{-1}), and Si-O-Si framework (1101, 798, and 468 cm^{-1})

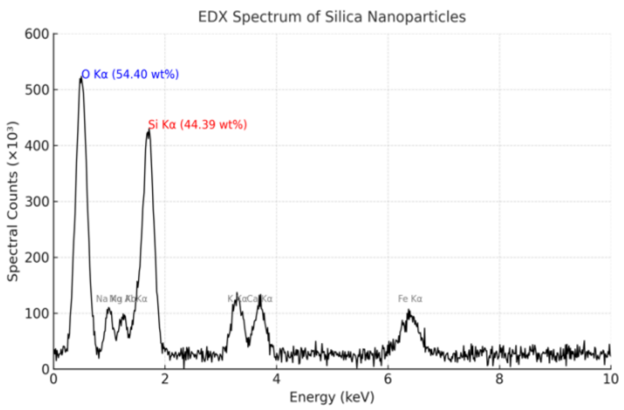

Figure 3. EDX (Energy Dispersive X-ray) spectrum of silica nanoparticle showing major peaks for Si and O with trace levels of Na, Mg, Al, K, Ca, dan Fe

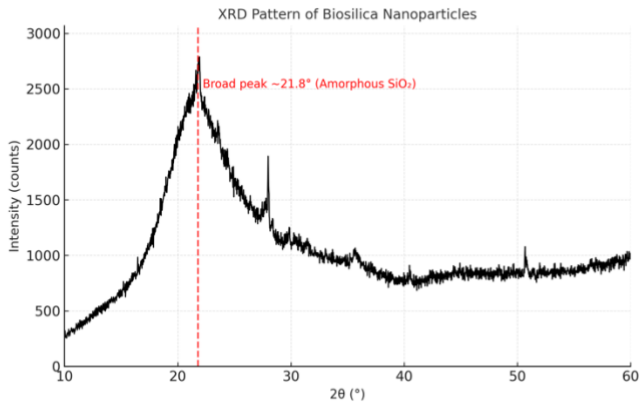

Figure 4. XRD (X-ray Diffraction) pattern of the synthesized biosilica nanoparticle

Table 1. Biochemical parameters of two black soybean cultivars under drought stress

Treatment	Prolin (μ mole g^{-1} FW)	H_2O_2 (μmol g^{-1} FW)	As. acid (ppm)	IC_{50} (ppm)
Malika + Non-AMF + Non-Biosilica nanoparticles	0.57 ^{a}±0.21	0.1635 ^{abc}±0.00021	114.64 ^{a}±38.15	15.44 ^{a}±2.46
Malika + Non-AMF + Biosilica nanoparticles 50	1.86 ^{ab}±1.48	0.1642 ^{c}±0.00030	125.58 ^{a}±37.10	15.29 ^{a}±3.28
Malika + Non-AMF + Biosilica nanoparticles 100	2.26 ^{ab}±0.38	0.1636 ^{abc}±0.00048	115.73 ^{a}±41.42	15.30 ^{a}±4.01
Malika + Non-AMF + Biosilica nanoparticles 150	1.33 ^{ab}±0.66	0.1636 ^{abc}±0.00036	109.21 ^{a}±22.66	14.55 ^{a}±4.33
Malika + Non-AMF + Biosilica nanoparticles 200	1.60 ^{ab}±2.59	0.1637 ^{abc}±0.00088	114.95 ^{a}±30.43	14.92 ^{a}±3.55
Malika + AMF + Non-Biosilica nanoparticles	1.29 ^{ab}±0.94	0.1642 ^{c}±0.00011	146.66 ^{a}±38.79	16.50 ^{a}±3.94
Malika + AMF + Biosilica nanoparticles 50	3.25 ^{ab}±1.02	0.1642 ^{c}±0.00053	108.67 ^{a}±37.00	14.01 ^{a}±2.18
Malika + AMF + Biosilica nanoparticles 100	3.06 ^{ab}±2.03	0.1636 ^{abc}±0.00031	115.57 ^{a}±33.37	16.94 ^{a}±0.74
Malika + AMF + Biosilica nanoparticles 150	0.62 ^{a}±0.44	0.1636 ^{abc}±0.00055	142.47 ^{a}±38.35	19.33 ^{a}±5.45
Malika + AMF + Biosilica nanoparticles 200	2.28 ^{ab}±1.55	0.1632 ^{ab}±0.00018	148.21 ^{a}±22.51	19.27 ^{a}±4.77
Detam 2 + Non-AMF + Non Biosilica nanoparticles	4.58 ^{b}±0.76	0.1642 ^{c}±0.00037	120.46 ^{a}±21.01	15.22 ^{a}±0.54
Detam 2+ Non-AMF + Biosilica nanoparticles 50	5.00 ^{b}±5.14	0.1636 ^{abc}±0.00047	137.67 ^{a}±34.90	14.48 ^{a}±0.17
Detam 2 + Non-AMF + Biosilica nanoparticles 100	2.58 ^{ab}±2.45	0.1636 ^{abc}±0.00024	139.99 ^{a}±11.64	18.61 ^{a}±4.97
Detam 2+ Non-AMF + Biosilica nanoparticles 150	1.95 ^{ab}±1.88	0.1636 ^{abc}±0.00035	138.44 ^{a}±31.13	14.86 ^{a}±0.84
Detam 2 + Non-AMF + Biosilica nanoparticles 200	0.46 ^{a}±0.15	0.1640 ^{abc}±0.0011	146.58 ^{a}±42.10	45.06 ^{b}±21.60
Detam 2 + AMF + Non-Biosilica nanoparticles	3.43 ^{ab}±1.66	0.1635 ^{abc}±0.00058	111.23 ^{a}±20.02	15.39 ^{a}±1.77
Detam 2 + AMF + Biosilica nanoparticles 50	4.71 ^{b}±2.66	0.1641 ^{bc}±0.00066	114.57 ^{a}±40.26	23.10 a±12.29
Detam 2+ AMF + Biosilica nanoparticles 100	0.44 ^{a}±0.51	0.1636 ^{abc}±0.00031	132.55 ^{a}±25.46	28.74 ^{a}±20.53
Detam 2 + AMF + Biosilica nanoparticles 150	0.65 ^{a}±0.39	0.1631 ^{a}±0.00012	102.86 ^{a}±32.17	16.56 ^{a}±2.73
Detam 2 + AMF + Biosilica nanoparticles 200	1.96 ^{ab}±2.22	0.1637 ^{abc}±0.00043	112.55 ^{a}±55.09	16.43 ^{a}±2.04

Note: Values represent mean±SD (n = 3). Different letters within a column indicate significant differences at $p<0.05$ according to Duncan's Multiple Range Test (DMRT). Biosilica nanoparticles concentration (0, 50, 100, 150, 200 ppm)

Root development responses

Root system development (Figures 5-6) was significantly influenced by cultivar, AMF inoculation, and biosilica nanoparticle concentration; with the strongest effect at 21 DAP. Detam 2 generally exhibited a tendency toward longer and more voluminous roots than Malika, particularly under AMF inoculation combined with 150-200 ppm biosilica nanoparticles. The interaction between AMF and biosilica nanoparticles enhanced root elongation and branching, improving water and nutrient uptake under drought stress (Cheng et al. 2021; Sharifian et al. 2022). By 28 DAP, root elongation reached its peak with a maximum root length of 37 cm observed in Detam 2 (Figure 5) and the highest root volume of 4.30 cm^3 in Malika (Figure 6). However, these differences were not statistically significant ($p>0.05$), likely because uninoculated plants grown under non-sterile field conditions may have experienced background AMF colonization. Notably, at 21 DAP, a significant cultivar × AMF × Biosilica nanoparticle interaction was detected: when both cultivars were inoculated with AMF and supplied with 200 ppm biosilica nanoparticles, Detam 2 exhibited a greater root volume (3.17 cm^3) and longer maximum root length (31.33 cm) than Malika (1.00 cm^3 and 14.67 cm, respectively). These stage-dependent and genotype-specific responses reinforce our primary conclusion that AMF, particularly when combined with an optimal biosilica nanoparticle concentration, promote root development under drought stress conditions.

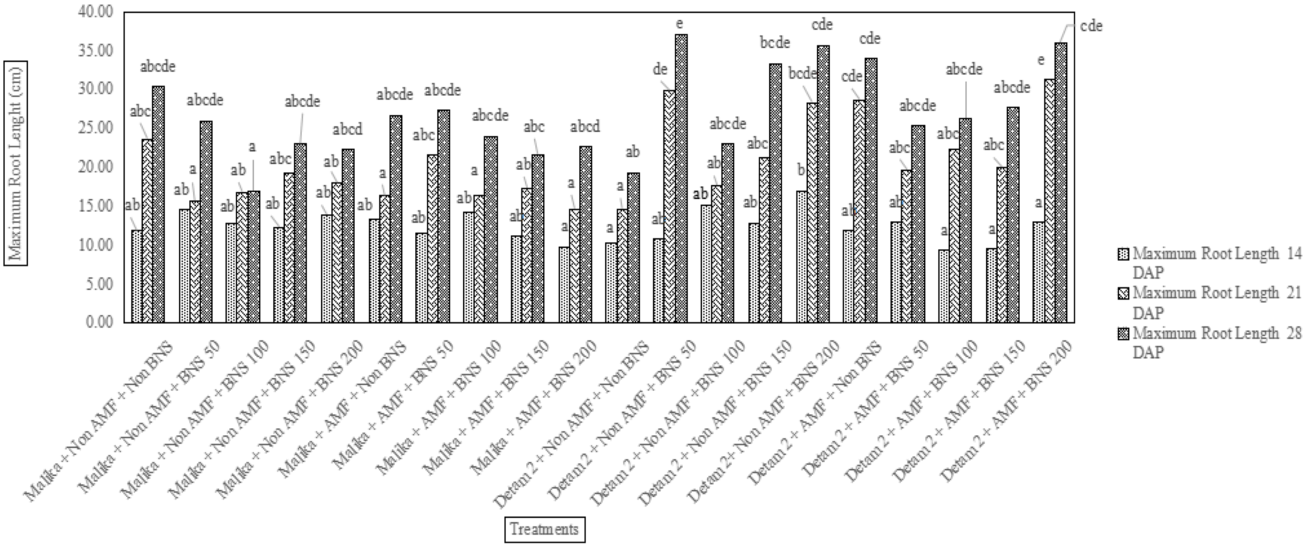

Figure 5. Effect of biosilica nanoparticle concentration and Arbuscular Mycorrhizal Fungi (AMF) inoculation on maximum root length of two black soybean cultivars at 14, 21, and 28 DAP. Different letters above the bars represent significant differences according to Duncan's Multiple Range Test (DMRT, p<0.05, n = 3)

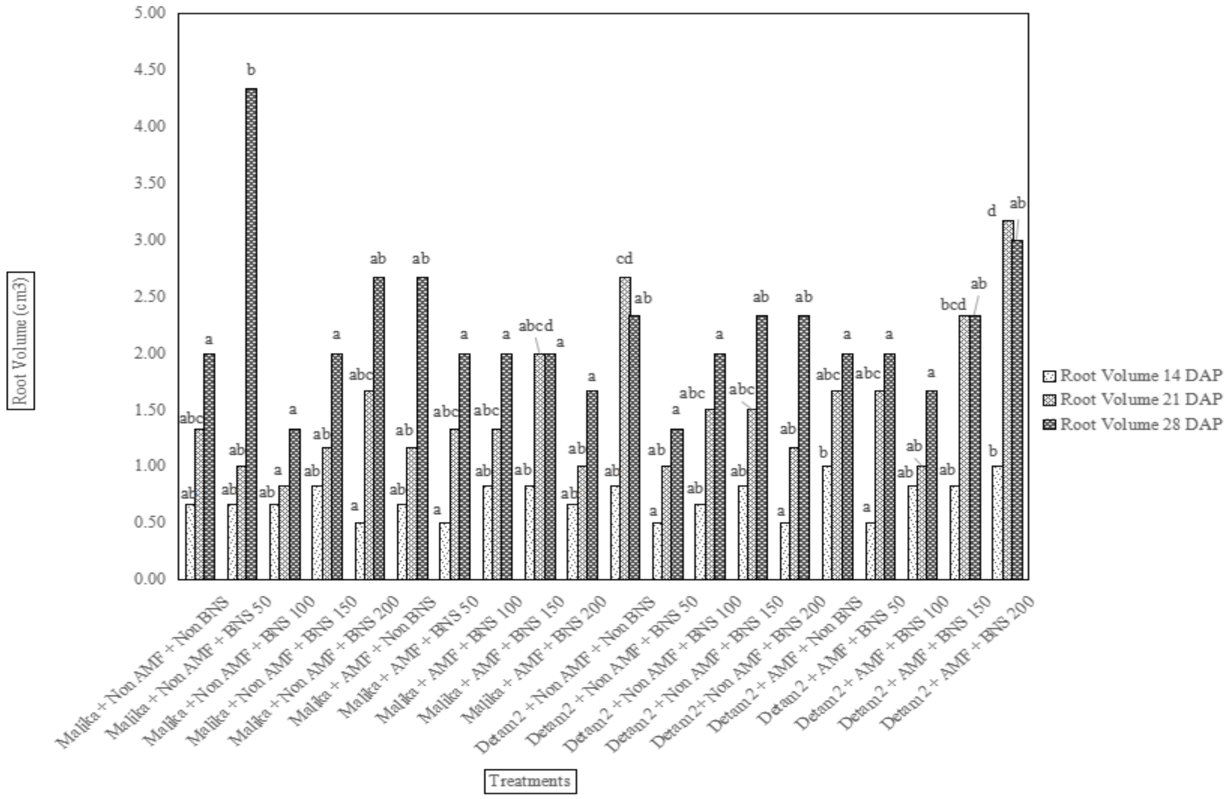

Figure 6. Effect of biosilica nanoparticle concentration and Arbuscular Mycorrhizal Fungi (AMF) inoculation on maximum root length of two black soybean cultivars at 14, 21, and 28 DAP. Different letters above the bars represent significant differences according to Duncan's Multiple Range Test (DMRT, p<0.05, n = 3)

Correlation analysis of biochemical parameters

A correlation test was performed to measure the strength of the relationship between biochemical parameters. Correlation analysis (Table 2) further elucidated these relationships among biochemical parameters. Proline content showed a weak negative correlation with IC_{50} (r = -0.205), suggesting that higher proline accumulation was associated with stronger antioxidant capacity. Although the correlation between proline, ascorbic acid, and H_2O_2 was non-significant, the negative direction indicated complementary antioxidant pathways acting to reduce oxidative stress.

Table 2. Correlation analysis of biochemical parameters

	Proline	H_2O_2	Ascorbic acid	IC_{50}
Proline	1			
H_2O_2	0.167 (p = 0.202)	1		
Ascorbic acid	-0.38 (p = 0.775)	0.048 (p = 0.715)	1	
IC_{50}	-0.205 (p = 0.116)	-0.166 (p = 0.204)	0.160 (p = 0.223)	1

Note: +: Positive correlation, -: Negative correlation, *: Correlation is significant at $p<0.05$ level (2-tailed), n = 3

Taken together, the integrated findings from biochemical responses (Table 1), root development (Figures 5 and 6), and correlation patterns (Table 2) demonstrate that AMF and biosilica nanoparticles acted synergistically to enhance drought tolerance in black soybean. Increased proline and ascorbic acid levels were associated with lower H_2O_2 accumulation and higher antioxidant efficiency, reflecting improved redox regulation. These biochemical adjustments were accompanied by enhanced root growth and volume, particularly under AMF inoculation, indicating that drought resilience results from coordinated osmotic, antioxidant, and morphological adaptations operating in a genotype-specific response.

Discussion

Silica (SiO_2) has long been applied in agriculture for enhancing plant growth and improving productivity under abiotic stress (Sangeetha et al. 2017). Nanomaterial-based fertilizers are increasingly favored because of their efficiency and reduced environmental impact (Amin et al. 2023). Our characterization data confirms that the synthesized rice-husk-derived bionanosilica possesses structural and physicochemical properties suitable for agricultural applications. TEM analysis revealed an average particle size of 58.31 nm, EDX confirms high purity of 98.79% by mass, FTIR spectra show characteristic silanol bands and water adsorption at 3435 cm^{-1} and 1630 cm^{-1}, along with Si-O-Si stretching at 1101, 798, and 468 cm^{-1}, and XRD analysis identified an amorphous structure with a 2θ peak at 21.8°. According to (Sankar et al. 2016) and (Dang et al. 2018), slightly larger nanoparticle sizes are obtained from differences in calcination equipment. The 1N HCl extraction achieves high purity, demonstrating effective removal of metal ions (De Valgaz et al. 2025). The amorphous form offers advantages for sustainable agriculture, including environmental safety, high surface area, improved nutrient binding, and rapid plant uptake under stress (Goswami et al. 2022). Thus, utilizing rice husk-derived biosilica nanoparticles not only contributes technologically but also aligns with sustainable agricultural practices. This characterization was directly quantified, whereas the subsequent physiological mechanisms discussed below are inferred from observed biochemical and morphological responses rather than direct molecular measurements.

The synergistic interaction between AMF and biosilica nanoparticles may involve concurrent improvements in redox balance and root development, as inferred from reduced H_2O_2 accumulation and enhanced root development during vegetative stages. This agrees with reports by Soliman et al. (2025), who demonstrated improved drought resilience through simultaneous AMF inoculation and biosilica nanoparticle application. Likewise, Begum et al. (2023) observed that such combinations were most effective at early growth stages. The exact biochemical processes, like enzymatic antioxidant regulation, were not directly measured, but the lower levels of H_2O_2 and better growth parameters suggest that cellular redox stability was indirectly improved (Sachdev et al. 2021). This synergy highlights the complementary role of AMF in improving water and nutrient uptake, and of biosilica nanoparticles in supporting cellular redox stability, which may indirectly contribute to membrane protection, forming an eco-friendly strategy for legume drought tolerance.

The genotypic differences can be explained by contrasting biochemical and morphological strategies, as supported by ANOVA, effect size, DMRT, and correlation analysis, which were observed between Malika and Detam 2, strongly supported by ANOVA and effect size across biochemical and morphological traits. Malika maintained stable H_2O_2 levels across treatment, consistent with the large effect size of biosilica nanoparticle (η^2 = 0.24) and small but significant contribution from AMF (p = 0.025; η^2 = 0.01)—those reflecting biochemical tolerance based on oxidative regulation. In contrast, Detam 2 showed greater proline accumulation (Biosilica nanoparticle p = 0.019; η^2 = 0.25; Cultivar×Biosilica nanoparticle p = 0.031; η^2 = 0.23) and more pronounced root elongation and root volume expansion (Root Length 21 DAP: p = 0.001, η^2 = 0.23; Root Volume 21 DAP: p = 0.125, η^2 = 0.16) under combined biosilica nanoparticle and AMF. It suggests a morphological adaptation strategy. Successful AMF colonization confirmed the establishment of functional symbiosis under the experimental conditions (Supplementary Tables 3 and 7; Supplementary Figures 1 and 2). The slightly higher colonization observed in Detam *2* suggests genotypic variation in AMF-root compatibility, which may influence the strength of the symbiotic response under drought stress. Although Detam 2 accumulates more proline, this may indicate greater cellular dehydration rather than superior tolerance (Bandurska et al. 2017). Higher biosilica nanoparticle doses (150-200 ppm) decrease proline content in Detam 2, suggesting that stress alleviation reduced osmolyte accumulation demand (Etesami et al. 2022). The main effect of AMF was small (η^2 = 0.003) for ascorbic acid content, but it had a significant effect on the interaction between cultivar and biosilica nanoparticle (p = 0.036; η^2 = 0.11), which means that AMF did not work alone but changed how antioxidants worked depending on the genotype. In Malika, this interaction manifested as increased ascorbic acid accumulation following AMF inoculation, reinforcing the role of mycorrhiza in enhancing non-enzymatic antioxidant activity and maintaining redox homeostasis. Meanwhile, lower IC_{50} values in Malika compared to Detam 2 indicate stronger total antioxidant capacity, supporting its efficiency in reactive oxygen species scavenging under combined treatments. Together, these genotype-dependent adjustments, supported by a large effect size in oxidative (H_2O_2), osmotic (proline), and morphological root traits, alongside moderate interaction for ascorbic acid, highlight the complementary biochemical and structural strategies of drought adaptation. This pattern aligns with the integrated tolerance model described by Kamau et al. (2021), where contrasting genotypes achieve resilience through distinct but coordinated redox and osmotic regulatory pathways.

The correlation analysis further strengthens the proposed synergistic mechanism between AMF and biosilica nanoparticles. A weak but negative correlation between proline and IC_{50} (r = -0.205) suggests that osmolyte accumulation modestly enhances antioxidant activity (Papagiouvannis et al. 2024). Even though higher proline is associated with reduced H_2O_2 levels (Tiika et al. 2023). This research reports a weak positive correlation and non-significant (r = 0.167), indicating that proline accumulation alone cannot fully explain variation in H_2O_2 levels. The balance between enzymatic (e.g., SOD, CAT, APX) and non-enzymatic antioxidants may differ among genotypes (Khan et al. 2025). A weak positive correlation between ascorbic acid and IC_{50} (r = 0.160) indicates that increases in ascorbate content were not directly associated with higher total antioxidant efficiency. This study suggests that while ascorbic acid contributes to the overall antioxidant pool, it is not the primary determinant of total ROS scavenging capacity. This observation aligns with previous findings indicating that enzymatic antioxidants such as CAT, APX, and POD play more dominant roles in ROS detoxification (Seminario et al. 2017). Likewise, the non-significant correlation between H_2O_2 and ascorbic acid supports the interpretation that H_2O_2 detoxification is mainly driven by enzymatic pathways rather than non-enzymatic antioxidants. The negative association between proline and ascorbic acid (r = -0.38) suggests a physiological trade-off between osmolyte accumulation and antioxidant metabolite production (Mahmud et al. 2023; Khan et al. 2024). These weak correlations collectively indicate that drought tolerance in black soybean involves multiple independent yet coordinated mechanisms balancing osmotic regulation, ROS detoxification, and root plasticity.

Collectively, the findings of this study suggest that black soybean cultivars employ dual drought adaptation pathways mediated by the interaction of AMF and biosilica nanoparticles. In Malika, drought tolerance was primarily associated with antioxidant-based osmotic adjustment, reflected by higher ascorbic acid content, stronger DPPH radical scavenging activity, and lower hydrogen peroxide (H_2O_2) accumulation. Meanwhile, Detam 2 exhibited a morphological adaptation pathway, supported by significant increases in root length and root volume, particularly at 21 DAP when AMF inoculation was combined with 200 ppm biosilica nanoparticles and accompanied by elevated proline accumulation. The higher proline levels in Detam 2 likely contributed to both osmotic regulation and root tissue development under drought stress. These results indicate that Malika relies more on biochemical antioxidant defense, whereas Detam 2 integrates osmotic and morphological mechanisms, illustrating complementary strategies that jointly enhance drought tolerance in black soybean cultivars.

The broader effects of using show how important biosafety and environmental sustainability are. Although nanosilica application can enhance plant growth response and yield, the response differs among species. Long-term application practices need to consider the correct dosage due to its potential phytotoxicity (Kumar et al. 2019), impact on soil microbes (Sharma and Kumar 2024), as its behavior is shaped by its characteristics and interactions with the soil environment (Usman et al. 2020). However, the use of biological resources such as bacteria, plants, and agricultural waste to produce nanomaterials has recently received substantial attention. This strategy is different from traditional ones because it is more adaptable to changing economy conditions and has less of a negative effect on the environment (Chakroborty et al. 2023).

While this study provides comprehensive physiological and statistical evidence, several limitations remain. Enzymatic antioxidants such as CAT, SOD, and APX were not measured, and some parameters exhibited relatively large standard deviations, reflecting natural biological variability under greenhouse conditions. The experiment was conducted under controlled greenhouse conditions with a relatively short observation period, which limits the generalizability of the findings to long-term field conditions. Accordingly, future research should include the quantification of enzymatic antioxidant activity, AMF colonization rate, and extended field trials to confirm whether vegetative-stage tolerance contributes to yield performance. A dose-response analysis is essential to assess potential phytotoxicological effects of nanosilica application. Moreover, subsequent investigation utilizing transcriptomic analysis and high-resolution root imaging is recommended to validate whether specific pathways regulate the identified biochemical and morphological responses.

In conclusion, this study demonstrated that the combined application of bio-silica nanoparticles and Arbuscular Mycorrhizal Fungi (AMF) effectively enhanced drought tolerance in black soybean cultivars Malika and Detam 2. The integration of AMF symbiosis and bio-silica treatment improved root development and antioxidant activity under drought conditions. Malika exhibited stronger biochemical tolerance through reduced hydrogen peroxide (H_2O_2) accumulation, while Detam 2 showed significant improvement in root development at 21 DAP when AMF inoculation was combined with 200 ppm biosilica nanoparticle. These findings emphasize that integrating biosilica nanoparticles and AMF enhances both forms of drought adaptation, providing a balanced framework for improving legume resilience under dryland conditions.

However, the experiment was limited to short-term greenhouse conditions and did not assess soil microbiome dynamics, enzyme activity, or long-term bio-silica accumulation effects. These constraints may have restricted the full understanding of plant-microbe nanomaterial interactions. Future studies should include multi-season and field-scale evaluations, molecular and enzymatic analyses to confirm stress response pathways, and investigation of optimal nanoparticle dosages under diverse soil conditions.

Integrating bio-silica and AMF applications into sustainable dryland farming systems could significantly improve legume productivity and resilience to climate-induced water stress.

ACKNOWLEDGEMENTS

This research was supported by the Indonesia Education Scholarship (*Beasiswa Pendidikan Indonesia*, BPI) from the Ministry of Higher Education, Science, and Technology through the Center for Financing and Assessment of Higher Education (PPAPT) and the Indonesia Endowment Fund for Education Agency (LPDP). The scholarship recipient identification number is 202209091593.

REFERENCES

Abdo RA, Hazem MM, El-Assar AE-M, Saudy HS, El-Sayed SM. 2024. Efficacy of nano-silicon extracted from rice husk to modulate the physio-biochemical constituents of wheat for ameliorating drought tolerance without causing cytotoxicity. Beni-Suef Univ J Basic Appl Sci 13: 75. DOI: 10.1186/s43088-024-00529-2.

Amin M, Juita N, Asnawi. 2023. Application of nano silica fertilizer in agricultural sustainability (a review). IOP Conf Ser: Earth Environ Sci 1230: 012063. DOI: 10.1088/1755-1315/1230/1/012063.

Arya H, Singh MB, Bhalla PL. 2021. Towards developing drought-smart soybeans. Front Plant Sci 12: 750664. DOI: 10.3389/fpls.2021.750664.

Asadullah, Kalhoro SA, Wajid F, Iqbal A, Sultan, Abdul W, Rashid M, Shah SRU. 2024. Exploring the variability of root system architecture under drought stress in heat-tolerant spring-wheat lines. Plant Soil 502: 103-119. DOI: 10.1007/s11104-024-06795-4.

Badan Pusat Statistik Boyolali. 2022. Produksi jagung, kedelai, kacang tanah, kacang hijau, ubi kayu, ubi jalar di Kabupaten Boyolali (ton) 2020. https://boyolalikab.bps.go.id/id. [Indonesian]

Balitkabi. 2024. Deskrispsi Varietas Unggul Kedelai 1918-2022. Badan Standardisasi Instrumen Pertanian, Kementerian Pertanian, Malang. [Indonesian]

Bandurska H, Niedziela J, Pietrowska-Borek M, Nuc K, Chadzinikolau T, Radzikowska D. 2017. Regulation of proline biosynthesis and resistance to drought stress in two barley (*Hordeum vulgare* L.) genotypes of different origin. Plant Physiol Biochem 118: 427-437. DOI: 10.1016/j.plaphy.2017.07.006.

Bates LS, Waldren RP, Teare ID. 1973. Proline analysis. Plant Soil 39: 205-207. DOI: 10.1007/bf00018060.

Begum N, Xiao Y, Wang L, Li D, Irshad A, Zhao T. 2023. Arbuscular mycorrhizal fungus *Rhizophagus irregularis* alleviates drought stress in soybean with overexpressing the GmSPL9d gene by promoting photosynthetic apparatus and regulating the antioxidant system. Microbiol Res 273: 127398. DOI: 10.1016/j.micres.2023.127398.

Bhartiya A, Aditya JP, Pal RS, Chandra N, Kant L, Pattanayak A. 2020. *Bhat* (Black soybean): A traditional legume with high nutritional and nutraceutical properties from NW Himalayan region of India. Indian J Tradit Knowl 19 (2): 307-319. DOI: 10.56042/ijtk.v19i2.35346.

Bhat JA, Rajora N, Raturi G, Sharma S, Dhiman P, Sanand S, Shivaraj SM, Sonah H, Deshmukh R. 2021. Silicon nanoparticles (SiNPs) in sustainable agriculture: Major emphasis on the practicality, efficacy and concerns. Nanoscale Adv 3: 4019-4028. DOI: 10.1039/d1na00233c.

Chakroborty S, Pal K, Nath N, Singh V, Barik A, Soren S, Panda P, Asthana N, Kyzas GZ. 2023. Sustainable synthesis of multifunctional nanomaterials from rice wastes: A comprehensive review. Environ Sci Pollut Res Intl 30 (42): 95039-95053. DOI: 10.1007/s11356-023-29235-9.

Chandrasekaran M. 2022. Arbuscular mycorrhizal fungi mediated alleviation of drought stress via non-enzymatic antioxidants: A meta-analysis. Plants 11 (19): 2448. DOI: 10.3390/plants11192448.

Cheng S, Zou Y-N, Kuča K, Hashem A, Abd-Allah EF, Wu Q-S. 2021. Elucidating the mechanisms underlying enhanced drought tolerance in plants mediated by arbuscular mycorrhizal fungi. Front Microbiol 12: 809473. DOI: 10.3389/fmicb.2021.809473.

Chowdhary NA, Songachan LS. 2025. Boosting sustainable agriculture by arbuscular mycorrhizal fungi under abiotic stress conditions. Plant Stress 17: 100945. DOI: 10.1016/j.stress.2025.100945.

Cohen J. 1988. Statistical Power Analysis for the Behavioral Sciences. 2nd eds. Academic Press, New York.

Dang NTT, Nguyen TTA, Phan TD, Tran H, Dang PV, Nguyen HQ. 2018. Synthesis of silica nanoparticles from rice husk ash. VNUHCM J Sci Technol Dev 20 (K7): 50-54. DOI: 10.32508/stdj.v20ik7.1211.

Darmanti S, Santosa, Dewi K, Nugroho LH. 2016. Antioxidative defenses of soybean (*Glycine max* (L.) Merr. cv. Grobogan) against purple nutsedge (*Cyperus rotundus* L.) interference during drought stress. J Anim Plant Sci 26 (1): 225-232.

De Valgaz APF, Cajas GS, Fermín AR. 2025. From rice husk to graphene: Exploring the effect of calcination and leaching. In: Inga Ortega EM, García Herranz N, Robles-Bykbaev VE, Gallego Diaz E (eds). Systems, Smart Technologies, and Innovation for Society. CITIS 2024. Lecture Notes in Networks and Systems. Springer, Cham. DOI: 10.1007/978-3-031-87065-1_25.

Etesami H, Noori F, Jeong BR. 2022. Directions for future research to use silicon and silicon nanoparticles to increase crops tolerance to stresses and improve their quality. In: Etesami H, Al Saeedi AH, El-Ramady H, Fujita M, Pessarakli M, Hossain MA (eds). Silicon and Nano-silicon in Environmental Stress Management and Crop Quality Improvement: Progress and Prospects. Academic Press, Cambridge. DOI: 10.1016/B978-0-323-91225-9.00015-7.

Goswami P, Mathur J, Srivastava N. 2022. Silica nanoparticles as novel sustainable approach for plant growth and crop protection. Heliyon 8 (7): e09908. DOI: 10.1016/j.heliyon.2022.e09908.

Guo C, Zhu L, Sun H, Han Q, Wang S, Zhu J, Zhang Y, Zhang K, Bai Z, Li A, Liu L, Li C. 2024. Evaluation of drought-tolerant varieties based on root system architecture in cotton (*Gossypium hirsutum* L.). BMC Plant Biol 24 (1): 127. DOI: 10.1186/s12870-024-04799-x.

Hasanuzzaman M, Parvin K, Anee TI, Masud AAC, Nowroz F. 2022. Salt stress responses and tolerance in soybean. In: Hasanuzzaman M, Nahar K (eds). Plant Stress Physiology-Perspectives in Agriculture. IntechOpen, Croatia. DOI: 10.5772/intechopen.102835.

Herawati N, Hadiawati L, Zulhaedar F. 2021. Optimum dosage of rice husk-based silicon foliar spray to improve yield of soybean grown on irrigated lowland. IOP Conf Ser: Earth Environ Sci 752: 012032. DOI: 10.1088/1755-1315/752/1/012032.

Hosseinifard M, Stefaniak S, Javid MG, Soltani E, Wojtyla Ł, Garnczarska M. 2022. Contribution of exogenous proline to abiotic stresses tolerance in plants: A review. Intl J Mol Sci 23 (9): 5186. DOI: 10.3390/ijms23095186.

Kamau NN, Kungu JB, Mugendi D. 2021. Effects of mycorrhizal and *Rhizobium* inoculation on soybean growth in acidic soils of Gatanga, Kenya. Cell Biol Dev 4 (1): 1-16. DOI: 10.13057/cellbioldev/v040101.

Kang B-H, Anderson CT, Arimura S-I et al. 2022. A glossary of plant cell structures: Current insights and future questions. Plant Cell 34 (1): 10-52. DOI: 10.1093/plcell/koab247.

Khan P, Abdelbacki AMM, Albaqami M, Jan R, Kim K-M. 2025. Proline promotes drought tolerance in maize. Biology 14 (1): 41. DOI: 10.3390/biology14010041.

Khan TA, Ahmad A, Saeed T, Yusuf M, Faisal M, Alatar AA. 2024. Investigating the influence of selenium and epibrassinolide on antioxidant activity, proline accumulation, and protein expression profiles in wheat plants experiencing heat and drought stress. Front Plant Sci 15: 1441483. DOI: 10.3389/fpls.2024.1441483.

Kowitcharoen L, Wongs-Aree C, Setha S, Komkhuntod R, Kondo S, Srilaong V. 2018. Pre-harvest drought stress treatment improves antioxidant activity and sugar accumulation of sugar apple at harvest and during storage. Agric Nat Resour 52 (2): 146-154. DOI: 10.1016/j.anres.2018.06.003.

Kumar A, Gupta K, Dixit K, Mishra K, Srivastava S. 2019. A review on positive and negative impacts of nanotechnology in agriculture. Intl J Environ Sci Technol 16: 2175-2184. DOI: 10.1007/s13762-018-2119-7.

Lee CW, Mahendra S, Zodrow K, Li D, Tsai Y-C, Braam J, Alvarez PJJ. 2010. Developmental phytotoxicity of metal oxide nanoparticles to *Arabidopsis thaliana*. Environ Toxicol Chem 29 (3): 669-675. DOI: 10.1002/etc.58.

Lismont C, Revenco I, Li H, Costa CF, Lenaerts L, Hussein MAF, De Bie J, Knoops B, Van Veldhoven PP, Derua R, Fransen M. 2022. Peroxisome-derived hydrogen peroxide modulates the sulfenylation profiles of key redox signaling proteins in Flp-In T-REx 293 cells. Front Cell Dev Biol 10: 888873. DOI: 10.3389/fcell.2022.888873.

Luan X, Bommarco R, Scaini A, Vico G. 2021. Combined heat and drought suppress rainfed maize and soybean yields and modify irrigation benefits in the USA. Environ Res Lett 16: 064023. DOI: 10.1088/1748-9326/abfc76.

Maddalena R, Hall C, Hamilton A. 2019. Effect of silica particle size on the formation of Calcium Silicate Hydrate [C-S-H] using thermal analysis. Thermochim Acta 672: 142-149. DOI: 10.1016/j.tca.2018.09.003.

Mahmud S, Kamruzzaman M, Bhattacharyya S, Alharbi K, Abd El Moneim D, Mostofa MG. 2023. Acetic acid positively modulates proline metabolism for mitigating PEG-mediated drought stress in maize and Arabidopsis. Front Plant Sci 14: 1167238. DOI: 10.3389/fpls.2023.1167238.

Maliya I, Darmanti S, Suedy SWA. 2019. The content of chlorophyll and antioxidant activity of malabar plum (*Syzygium jambos*) leaves at different developmental stages. Biosaintifika 11 (2): 226-233. DOI: 10.15294/biosaintifika.v11i2.18419.

Mathur P, Roy S. 2020. Nanosilica facilitates silica uptake, growth and stress tolerance in plants. Plant Physiol Biochem 157: 114-127. DOI: 10.1016/j.plaphy.2020.10.011.

Moradtalab N, Hajiboland R, Aliasgharzad N, Hartmann TE, Neumann G. 2019. Silicon and the association with an arbuscular-mycorhizal fungus (*Rhizophagus clarus*) mitigate the adverse effects of drought stress on strawberry. Agronomy 9: 41. DOI: 10.3390/agronomy9010041.

Mwenye OJ, van Rensburg L, van Biljon A, van der Merwe R. 2016. The role of proline and root traits on selection for drought-stress tolerance in soybeans: A review. S Afr J Plant Soil 33 (4): 245-256. DOI: 10.1080/02571862.2016.1148786.

Nader AA, Hauka FIA, Afify AH, El-Sawah AM. 2024. Drought-tolerant bacteria and arbuscular mycorrhizal fungi mitigate the detrimental effects of drought stress induced by withholding irrigation at critical growth stages of soybean (*Glycine max*, L.). Microorganisms 12 (6): 1123. DOI: 10.3390/microorganisms12061123.

Naidu S, Pandey J, Mishra LC, Chakraborty A, Roy A, Singh IK, Singh A. 2023. Silicon nanoparticles: Synthesis, uptake and their role in mitigation of biotic stress. Ecotoxicol Environ Saf 255: 114783. DOI: 10.1016/j.ecoenv.2023.114783.

Papagiouvannis G, Theodosis-Nobelos P, Rekka EA. 2024. Trolox, ferulic, sinapic, and cinnamic acid derivatives of proline and GABA with antioxidant and/or anti-inflammatory properties. Molecules 29 (16): 3763. DOI: 10.3390/molecules29163763.

Poudel S, Vennam RR, Shrestha A, Reddy KR, Wijewardani NK, Reddy KN, Beemanahalli R. 2023. Resilience of soybean cultivars to drought stress during flowering and early-seed setting stages. Sci Rep 13 (1): 1227. DOI: 10.1038/s41598-023-28354-0.

Putra R, Waterman JM, Mathesius U, Wojtalewicz D, Powell JR, Hartley SE, Johnson SN. 2022. Benefits of silicon-enhanced root nodulation in a model legume are contingent upon rhizobial efficacy. Plant Soil 477: 201-217. DOI: 10.1007/s11104-022-05358-9.

Rakesh B, Chitdeshwari T, Mohanapriya G. 2024. Fascinating role of nanosilica in mitigating drought and nutrient stress - a review. Plant Stress 14: 100672. DOI: 10.1016/j.stress.2024.100672.

Rudenko NN, Vetoshkina DV, Marenkova TV, Borisova-Mubarakshina MM. 2023. Antioxidants of non-enzymatic nature: Their function in higher plant cells and the ways of boosting their biosynthesis. Antioxidants 12 (11): 2014. DOI: 10.3390/antiox12112014.

Sachdev S, Ansari SA, Ansari MI, Fujita M, Hasanuzzaman M. 2021. Abiotic stress and reactive oxygen species: Generation, signaling, and defense mechanisms. Antioxidants 10 (2): 277. DOI: 10.3390/antiox10020277.

Sangeetha J, Thangadurai D, Hospet R et al. 2017. Nanoagrotechnology for soil quality, crop performance and environmental management. In: Prasad R, Kumar M, Kumar V (eds). Nanotechnology: An Agricultural Paradigm. Springer, Singapore. DOI: 10.1007/978-981-10-4573-8_5.

Sankar S, Sharma SK, Kaur N, Lee B, Kim DY, Lee S, Jung H. 2016. Biogenerated silica nanoparticles synthesized from sticky, red, and brown rice husk ashes by a chemical method. Ceram Intl 42 (4): 4875-4885. DOI: 10.1016/j.ceramint.2015.11.172.

Seminario A, Song L, Zulet A, Nguyen HT, González EM, Larrainar E. 2017. Drought stress causes a reduction in the biosynthesis of ascorbic acid in soybean plants. Front Plant Sci 8: 1042. DOI: 10.3389/fpls.2017.01042.

Sharifian A, Mirzakhani A, Khaghani S, Kakhaki SFF. 2022. The combined use of silicon and arbuscular mycorrhizal fungus mitigate the adverse effects of drought stress on *Matthiola incana*. Notul Bot Horti Agrobot Cluj-Napoca 50: 12947. DOI: 10.15835/nbha50412947.

Sharma R, Kumar V. 2024. Nano-enabled agriculture for sustainable soil. Waste Manag Bull 2 (1): 152-161. DOI: 10.1016/j.wmb.2024.01.002.

Singh S, Singh P, Tomar RS, Sharma RA, Singh SK. 2022. Proline: A key player in biotic and abiotic stress in plants. In: Rani M, Chaudhary BS, Jamal S, Kumar P (eds). Towards Sustainable Natural Resources: Monitoring and Managing Ecosystem Biodiversity. Springer, Cham. DOI: 10.1007/978-3-031-06443-2_18.

Sitepu ME, Hariandi D, Septirosya T. 2024. Effectiveness test of local Arbuscular Mycorrhizal Fungi (AMF) and cocoa waste compost on the growth of cocoa seedlings (*Theobroma cacao* L.) in former mining sites. Jerami Indones J Crop Sci 6 (2): 55-62. DOI: 10.25077/jijcs.6.2.55-62.2024.

Soliman ERS, Abdelhameed RE, Metwally RA. 2025. Role of arbuscular mycorrhizal fungi in drought-resilient soybeans (*Glycine max* L.): Unraveling the morphological, physio-biochemical traits, and expression of polyamine biosynthesis genes. Bot Stud 66 (1): 9. DOI: 10.1186/s40529-025-00455-1.

Suciaty T, Purnomo D, Sakya AT, Supriyadi. 2018. The effect of nano-silica fertilizer concentration and rice hull ash doses on soybean (*Glycine max* (L.) Merrill) growth and yield. IOP Conf Ser: Earth Environ Sci 129: 012009. DOI: 10.1088/1755-1315/129/1/012009.

Tang H, Hassan MU, Feng L, Nawaz M, Shah AN, Qari SH, Liu Y, Miao J. 2022. The critical role of arbuscular mycorrhizal fungi to improve drought tolerance and nitrogen use efficiency in crops. Front Plant Sci 13: 919166. DOI: 10.3389/fpls.2022.919166.

Tiika RJ, Duan H, Yang H, Cui G, Tian F, He Y, Ma Y, Li Y. 2023. Proline metabolism process and antioxidant potential of *Lycium ruthenicum* Murr. in response to NaCl treatments. Intl J Mol Sci 24 (18): 13794. DOI: 10.3390/ijms241813794.

Usman M, Farooq M, Wakeel A, Nawaz A, Cheema SA, Ur Rehman H, Ashraf I, Sanaullah M. 2020. Nanotechnology in agriculture: Current status, challenges, and future opportunities. Sci Total Environ 721: 137778. DOI: 10.1016/j.scitotenv.2020.137778.

Velikova V, Yordanov I, Edreva A. 2000. Oxidative stress and some antioxidant systems in acid rain-treated bean plants: Protective role of exogenous polyamines. Plant Sci 151 (1): 59-66. DOI: 10.1016/S0168-9452(99)00197-1.

Wadas W. 2022. Possibility of increasing early crop potato yield with foliar application of silicon. Agron Sci 77 (2): 61-75. DOI: 10.24326/as.2022.2.6.

Wahab A, Muhammad M, Munir A, Abdi G, Zaman W, Ayaz A, Khizar C, Reddy SPP. 2023. Role of arbuscular mycorrhizal fungi in regulating growth, enhancing productivity, and potentially influencing ecosystems under abiotic and biotic stresses. Plants 12 (17): 3102. DOI: 10.3390/plants12173102.

Wei J, Liu L, Wei Z, Qin Q, Bai Q, Zhao C, Zhang S, Wang H. 2025. Silicon nano-fertilizer-enhanced soybean resilience and yield under drought stress. Plants 14 (5): 751. DOI: 10.3390/plants14050751.

Wei Y, Yang W, Yang Z. 2022. An excellent universal catalyst support-mesoporous silica: Preparation, modification and applications in energy-related reactions. Intl J Hydrogen Energy 47 (16): 9537-9565. DOI: 10.1016/j.ijhydene.2022.01.048.

SUPPLEMENTARY DATA

Supplementary Table 1. Recapitulation of ANOVA and effect size analysis in biochemical parameters

Parameters	Source	df	F	P value	Effect size (partial eta squared/η²)	Interpretation
H_2O_2	Cultivar	1	0.297	0.589	0.01	Small
	Biosilica nanoparticles	4	3.141	0.487	0.24	Large
	AMF	1	0.491	0.025	0.01	Small
	Cultivar X Biosilica nanoparticles	4	0.936	0.453	0.09	Medium
	Cultivar X AMF	1	0.648	0.426	0.16	Large
	Bionanosilika X AMF	4	0.629	0.644	0.59	Large
	Cultivar X Biosilica nanoparticles X AMF	4	1.962	0.119	0.16	Large
Prolin	Cultivar	1	2.498	0.122	0.06	Medium
	Biosilica nanoparticles	4	3.32	0.019	0.25	Large
	AMF	1	0.011	0.916	0.00	Small
	Cultivar X Biosilica nanoparticles	4	2.959	0.031	0.23	Large
	Cultivar X AMF	1	1.679	0.203	0.04	Small
	Bionanosilika X AMF	4	0.636	0.639	0.06	Medium
	Cultivar X Biosilica nanoparticles X AMF	4	0.436	0.782	0.04	Small
Ascorbic acid	Cultivar	1	0.03	0.864	0.001	Small
	Biosilica nanoparticles	4	0.101	0.753	0.01	Small
	AMF	1	0.128	0.971	0.003	Small
	Cultivar X Biosilica nanoparticles	4	4.705	0.036	0.11	Medium
	Cultivar X AMF	1	0.481	0.750	0.05	Small
	Bionanosilika X AMF	4	0.327	0.858	0.03	Small
	Cultivar X Biosilica nanoparticles X AMF	4	0.609	0.658	0.06	Medium
IC_{50}	Cultivar	1	5.43	0.025	0.12	Medium
	Biosilica nanoparticles	4	2.193	0.087	0.18	Large
	AMF	1	0.016	0.899	0.00	Small
	Cultivar X Biosilica nanoparticles	4	1.737	0.161	0.15	Large
	Cultivar X AMF	1	0.846	0.363	0.21	Large
	Bionanosilika X AMF	4	2.693	0.044	0.21	Large
	Cultivar X Biosilica nanoparticles X AMF	4	3.847	0.010	0.28	Large

Supplementary Table 2. Recapitulation of ANOVA and effect size analysis in root development parameters

Parameters	Source	df	F	P value	Effect size (partial eta squared/η²)	Interpretation
Root lenght 14 DAP	Cultivar	1	0.127	0.723	0.003	Small
	Biosilica nanoparticles	4	0.737	0.572	0.07	Medium
	AMF	1	3.155	0.083	0.07	Medium
	Cultivar X Biosilica nanoparticles	4	1.084	0.378	0.10	Medium
	Cultivar X AMF	1	0.231	0.634	0.01	Small
	Bionanosilika X AMF	4	1.264	0.300	0.11	Medium
	Cultivar X Biosilica nanoparticles X AMF	4	1.497	0.221	0.13	Medium
Root lenght 21 DAP	Cultivar	1	12.226	0.001	0.23	Large
	Biosilica nanoparticles	4	1.17	0.338	0.11	Medium
	AMF	1	0.038	0.847	0.00	Small
	Cultivar X Biosilica nanoparticles	4	1.957	0.12	0.16	Large
	Cultivar X AMF	1	1.26	0.268	0.03	Small
	Bionanosilika X AMF	4	0.464	0.761	0.04	Small
	Cultivar X Biosilica nanoparticles X AMF	4	3.793	0.010	0.28	Large
Root lenght 28 DAP	Cultivar	1	9.38	0.004	0.19	Large
	Biosilica nanoparticles	4	1.667	0.177	0.14	Large
	AMF	1	0.064	0.802	0.00	Small
	Cultivar X Biosilica nanoparticles	4	1.824	0.143	0.15	Large
	Cultivar X AMF	1	0.021	0.886	0.00	Small
	Bionanosilika X AMF	4	1.386	0.256	0.12	Medium
	Cultivar X Biosilica nanoparticles X AMF	4	1.957	0.120	0.16	Large
Root volume14 DAP	Cultivar	1	1.231	0.274	0.03	Small
	Biosilica nanoparticles	4	2.962	0.031	0.23	Large
	AMF	1	2.769	0.104	0.07	Medium
	Cultivar X Biosilica nanoparticles	4	1.038	0.399	0.09	Medium
	Cultivar X AMF	1	1.231	0.274	0.03	Small

	Bionanosilika X AMF	4	1.423	0.244	0.13	Medium
	Cultivar X Biosilica nanoparticles X AMF	4	0.269	0.896	0.03	Small
Root volume 21 DAP	Cultivar	1	6.782	0.013	0.15	Large
	Biosilica nanoparticles	4	1.968	0.118	0.16	Large
	AMF	1	2.331	0.135	0.06	Medium
	Cultivar X Biosilica nanoparticles	4	0.774	0.549	0.07	Medium
	Cultivar X AMF	1	0.395	0.533	0.01	Small
	Bionanosilika X AMF	4	1.927	0.125	0.16	Large
	Cultivar X Biosilica nanoparticles X AMF	4	3.137	0.025	0.24	Large
Root volume 28 DAP	Cultivar	1	0.278	0.601	0.01	Small
	Biosilica nanoparticles	4	0.756	0.56	0.07	Medium
	AMF	1	0.278	0.601	0.01	Small
	Cultivar X Biosilica nanoparticles	4	1.601	0.193	0.14	Medium
	Cultivar X AMF	1	0.993	0.325	0.02	Small
	Bionanosilika X AMF	4	0.399	0.808	0.04	Small
	Cultivar X Biosilica nanoparticles X AMF	4	1.835	0.141	0.16	Large

Supplementary Table 3. Recapitulation of ANOVA and effect size analysis in AMF colonization (%)

Source	df	F	P value	Effect size (partial eta squared/ η^2)	Interpretation
Cultivar	1	0.1297	0.262	0.03	Small
Biosilica nanoparticles	4	3.693	0.012	0.27	Large
AMF	1	12.236	0.01	0.23	Large
Cultivar X Biosilica nanoparticles	4	1.576	0.199	0.14	Large
Cultivar X AMF	1	0.099	0.755	0.002	Small
Bionanosilika X AMF	4	0.747	0.566	0.07	Medium
Cultivar X Biosilica nanoparticles X AMF	4	0.105	0.980	0.01	Small

Supplementary Table 4. Biochemical activity of Malika and Detam 2 with application of biosilica nanoparticle and mikorhiza under drought stress

Cultivars	Mikorhiza	Bionanosilika (ppm)	Prolin (μ mole g^{-1} FW)	H_2O_2 (μmol g^{-1} FW)	Ascorbic acid (ppm)	IC_{50} (ppm)
Malika	Non AMF	0	0.57 ^{a}±0.21	0.1635 ^{abc}±0.00021	114.64 ^{a}±38.15	15.44 ^{a}±2.46
		50	1.86 ^{ab}±1.48	0.1644 ^{c}±0.00030	125.58 ^{a}±37.10	15.29 ^{a}±3.28
		100	2.26 ^{ab}±0.38	0.1636 ^{abc}±0.00048	115.73 ^{a}±41.42	15.30 ^{a}±4.01
		150	1.33 ^{ab}±0.66	0.1636 ^{abc}±0.00036	109.21 ^{a}±22.66	14.55 ^{a}±4.33
		200	1.60 ^{ab}±2.59	0.1637 ^{abc}±0.00088	114.95 ^{a}±30.43	14.92 ^{a}±3.55
	AMF	0	1.29 ^{ab}±0.94	0.1643 ^{c}±0.00011	146.66 ^{a}±38.79	16.50 ^{a}±3.94
		50	3.25 ^{ab}±1.02	0.1642 ^{c}±0.00053	108.67 ^{a}±37.00	14.01 ^{a}±2.18
		100	3.06 ^{ab}±2.03	0.1636 ^{abc}±0.00031	115.57 ^{a}±33.37	16.94 ^{a}±0.74
		150	0.62 ^{a}±0.44	0.1635 ^{abc}±0.00055	142.47 ^{a}±38.35	19.33 ^{a}±5.45
		200	2.28 ^{ab}±1.55	0.1632 ^{ab}±0.00018	148.21^{a}± 22.51	19.27 ^{a}±4.77
Detam 2	Non AMF	0	4.58 ^{b}±0.76	0.1642 ^{c}±0.00037	120.46 ^{a}±21.01	15.22 ^{a}±0.54
		50	5.00 ^{b}±5.14	0.1636 ^{abc}±0.00047	137.67 ^{a}±34.90	14.48 ^{a}±0.17
		100	2.58 ^{ab}±2.45	0.1636 ^{abc}±0.00024	139.99 ^{a}±11.64	18.61 ^{a}±4.97
		150	1.95 ^{ab}±1.88	0.1636 ^{abc}±0.00035	138.44 ^{a}±31.13	14.86 ^{a}±0.84
		200	0.46 ^{a}±0.15	0.1640 ^{abc}±0.0011	146.58 ^{a}±42.10	45.06 ^{b}±21.60
	AMF	0	3.43 ^{ab}±1.66	0.1636 ^{abc}±0.00058	111.23 ^{a}±20.02	15.39 ^{a}±1.77
		50	4.71 ^{b}±2.66	0.1641 ^{bc}±0.00066	114.57 ^{a}±40.26	23.10 ^{a}±12.29
		100	0.44 ^{a}±0.51	0.1636 ^{abc}±0.00031	132.55 ^{a}±25.46	28.74 ^{a}±20.53
		150	0.65 ^{a}±0.39	0.1631 ^{a}±0.00012	102.86 ^{a}±32.17	16.56 ^{a}±2.73
		200	1.96 ^{ab}±2.22	0.1637 ^{abc}±0.00043	112.55 ^{a}±55.09	16.43 ^{a}±2.04
Cutivars			ns	ns	ns	*
AMF			ns	ns	ns	ns
Bionanosiika			*	*	ns	ns
Cutivars X AMF			ns	ns	*	ns
Cutivars X Bionanosilika			*	ns	ns	ns
Mikorhiza X Bionanosiika			ns	ns	ns	*
Cultivars X AMF X Bionanosiika			ns	ns	ns	*

Note: *: Substantially different according to the F test with α 5%, ns: Not significantly different. According to the DMRT test with α 5%, numbers in the same column that are followed by the same letter do not differ substantially

Supplementary Table 5. The maximum root length of Malika cultivar and Detam 2 cultivar under drought stress

Cultivars	Mikorhiza	Biosilica nanoparticle (ppm)	Maximum root length (cm)		
			14 DAP	21 DAP	28 DAP
Malika	Non AMF	0	11.83 ^{ab}±1.04	23.67 ^{abc}±5.13	30.33 ^{abcde}±5.69
		50	14.67 ^{ab}±4.04	15.67 ^{a}±7.64	26.00 ^{abcde}±9.54
		100	12.83 ^{ab}±2.47	16.83 ^{ab}±2.75	17.00 ^{a}±4.00
		150	12.33 ^{ab}±4.51	19.33 ^{abc}±4.93	23.00 ^{abcde}±8.89
		200	13.91 ^{ab}±1.23	18.00 ^{ab}±3.46	22.33 ^{abcd}±2.52
	AMF	0	13.33 ^{ab}±2.84	16.33 ^{a}±4.04	26.67 ^{abcde}±12.22
		50	11.50 ^{ab}±1.80	21.67 ^{abc}±5.51	27.33 ^{abcde}±7.09
		100	14.33 ^{ab}±3.33	16.33 ^{a}±2.52	24 ^{abcde}±3.00
		150	11.17 ^{ab}±3.79	17.33 ^{ab}±3.21	21.67 ^{abc}±2.31
		200	9.83 ^{a}±2.75	14.67 ^{a}±1.53	22.67 ^{abcd}±7.09
Detam 2	Non AMF	0	10.27 ^{a}±1.17	14.67 ^{a}±1.53	19.33 ^{ab}±3.06
		50	10.83 ^{ab}±2.47	29.83 ^{de}±14.37	37.00 ^{e}±12.77
		100	15.17 ^{ab}±3.55	17.67 ^{ab}±1.53	23.00 ^{abcde}±2.65
		150	12.83 ^{ab}±6.93	21.33 ^{abc}±5.13	33.33 ^{bcde}±9.07
		200	17.00 ^{b}±4.36	28.33 ^{bcde}±5.13	35.67 ^{cde}±2.52
	AMF	0	11.83 ^{ab}±3.33	28.67 ^{cde}±6.11	34 ^{cde}±5.57
		50	13.00 ^{ab}±0.50	19.67 ^{abc}±0.58	25.33 ^{abcde}±1.53
		100	9.33 ^{a}±3.21	22.33 ^{abc}±9.29	26.33 ^{abcde}±9.29
		150	9.50 ^{a}±1.32	20.00 ^{abc}±1.0	27.67 ^{abcde}±4.16
		200	13.00 ^{ab}±2.65	31.33 ^{e}±11.50	36.00 ^{de}±11.53
Cultivars			ns	*	ns
AMF			ns	ns	ns
Biosilica nanoparticle			ns	ns	*
Cultivars x AMF			ns	ns	ns
Cutivars x Biosilica nanoparticle			ns	ns	ns
Mychorrizae x Biosilica nanoparticle			ns	ns	ns
Cultivars x AMF x Biosilica nanoparticle			ns	*	ns

Note: *: Substantially different according to the F test with α 5%, ns: Not significantly different. According to the DMRT test with α 5%, numbers in the same column that are followed by the same letter do not differ substantially

Supplementary Table 6. Root volume of Malika cultivar and Detam 2 cultivar under drought stress

Cultivars	Mikorhiza	Biosilica nanoparticle (ppm)	Root volume (cm^3)		
			14 DAP	21 DAP	28 DAP
Malika	Non AMF	0	0.67 ^{ab}±0.29	1.33 ^{abc}±0.58	2.17 ^{a}±1.80
		50	0.67 ^{ab}±0.29	1.0 ^{ab}±0.00	4.3 ^{b}±2.52
		100	0.67 ^{ab}±0.29	0.83 ^{a}±0.29	1.33 ^{a}±0.58
		150	0.83 ^{ab}±0.29	1.17 ^{ab}±0.29	2.0 ^{a}±1.00
		200	0.5 ^{a}±0.00	1.67 ^{abc}±0.58	2.67 ^{ab}±0.58
	AMF	0	0.67 ^{ab}±0.29	1.17 ^{ab}±0.76	2.67 ^{ab}±2.08
		50	0.5 ^{a}±0.00	1.33 ^{abc}±0.58	2.0 ^{a}±1.00
		100	0.83 ^{ab}±0.29	1.33 ^{abc}±0.58	2.0 ^{a}±0.00
		150	0.83 ^{ab}±0.29	2.0 ^{abcd}±1.00	2.0 ^{a}±1.00
		200	0.67 ^{ab}±0.29	1.0 ^{ab}±0.00	1.67 ^{a}±1.15
Detam 2	Non AMF	0	0.83 ^{ab}±0.29	2.67 ^{cd}±0.58	2.33 ^{ab} ±0.58
		50	0.5 ^{a}±0.00	1.00 ^{ab}±0.5	1.33 ^{a}±0.58
		100	0.67 ^{ab}±0.29	1.5 ^{abc}±0.5	2.0 ^{a}±0.00
		150	0.83 ^{ab}±0.29	1.5 ^{abc}±0.5	2.33 ^{ab}±0.58
		200	0.5 ^{a}±0.00	1.17 ^{ab}±0.29	2.33 ^{ab}±0.58
	AMF	0	1.0 ^{b}±0.00	1.67 ^{abc}±1.15	2.0 ^{a}±1.00
		50	0.5 ^{a}±0.00	1.67 ^{abc}±0.58	2.0 ^{a}±0.00
		100	0.83 ^{ab}±0.29	1.0 ^{ab}±0.00	1.67 ^{a}±0.58
		150	0.83 ^{ab}±0.29	2.33 ^{bcd}±1.53	2.33 ^{ab}±0.58
		200	1.0 ^{b}±0.00	3.17 ^{d}±1.44	3.0 ^{ab}±1.73
Cultivars			ns	*	ns
AMF			*	ns	ns
Biosilica nanoparticle			*	ns	ns
Cultivars x AMF			ns	ns	ns
Cutivars x Biosilica nanoparticle			ns	ns	ns
Mychorrizae x Biosilica nanoparticle			ns	ns	ns
Cultivars x AMF x Biosilica nanoparticle			ns	*	ns

Note: *: Substantially different according to the F test with α 5%, ns: Not significantly different. According to the DMRT test with α 5%, numbers in the same column that are followed by the same letter do not differ substantially

Supplementary Table 7. AMF colonization of Malika cultivar and Detam 2 cultivar under drought stress

Cultivars	Mikorhiza	Biosilica nanoparticle (ppm)	AMF Colonization (%)
Malika	Non AMF	0	87.77bcd±3.87
		50	50.00 a±20.00
		100	80.00 bcd±17.32
		150	60.00 ab±30.00
		200	76.67 abcd±5.77
	AMF	0	95.83 d±7.22
		50	77.77 abcd±6.93
		100	93.33 cd±11.55
		150	73.33 abcd±30.55
		200	90.00 bcd±10.00
Detam 2	Non AMF	0	86.67 bcd±11.55
		50	73.33 abcd±25.17
		100	83.33 bcd±11.55
		150	63.33 abc±20.82
		200	83.33 bcd±20.82
	AMF	0	83.33 bcd±5.77
		50	96.67 d±5.77
		100	100.00 d±0.00
		150	80.00 bcd±10.00
		200	86.67 bcd±5.77
Cultivars			ns
AMF			*
Biosilica nanoparticle			*
Cultivars x AMF			ns
Cutivars x Biosilica nanoparticle			ns
AMF x Biosilica nanoparticle			ns
Cultivars x AMF x Biosilica nanoparticle			ns

Note: *: Substantially different according to the F test with α 5%, ns: Not significantly different. According to the DMRT test with α 5%, numbers in the same column that are followed by the same letter do not differ substantially

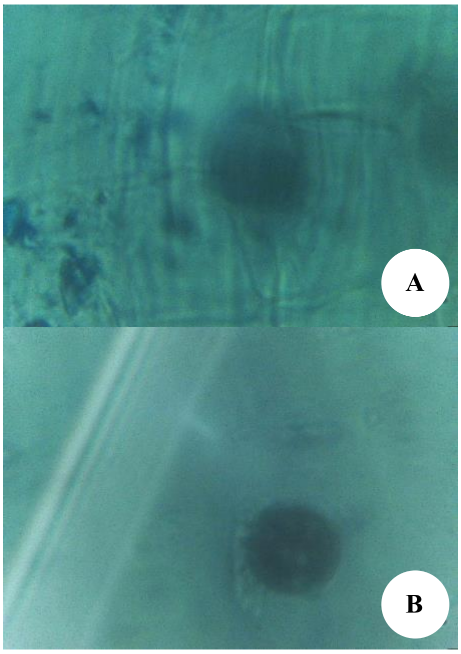

Supplementary Figure 1. Root colonization was also observed in Malika plants under the: A. Non-AMF treatment, and B. AMF treatment as confirmed by microscopic observation at 10×40 magnification

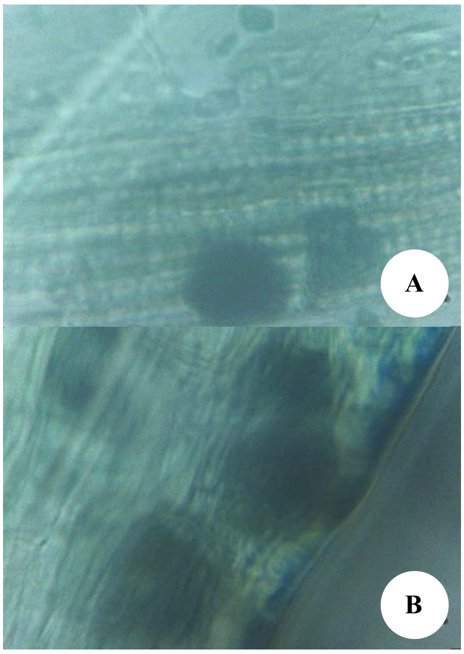

Supplementary Figure 2. Root colonization was also observed in Detam 2 plants under the under the: A. Non-AMF treatment, and B. AMF treatment as confirmed by microscopic observation at 10×40 magnification